Caveolar peroxynitrite formation impairs endothelial TRPV4 channels and elevates pulmonary arterial pressure in pulmonary hypertension

Zdravka Daneva[a], Corina Marziano[a], Matteo Ottolini[a,b], Yen-Lin Chen[a], Thomas M. Baker[a], Maniselvan Kuppusamy[a], Aimee Zhang[c], Huy Q. Ta[c], Claire E. Reagan[d], Andrew D. Mihalek[e], Ramesh B. Kasetti[f,g], Yuanjun Shen[h,i,j,k], Brant E. Isakson[a,l], Richard D. Minshall[m,n], Gulab S. Zode[f,g], Elena A. Goncharova[h,i,j,k], Victor E. Laubach[c], and Swapnil K. Sonkusare[a,b,l,1]

[a]Robert M. Berne Cardiovascular Research Center, University of Virginia, Charlottesville, VA 22908; [b]Department of Pharmacology, University of Virginia, Charlottesville, VA 22908; [c]Department of Surgery, University of Virginia, Charlottesville, VA 22908; [d]Department of Biomedical Engineering, University of Virginia, Charlottesville, VA 22908; [e]Department of Pulmonary and Critical Care Medicine, University of Virginia, Charlottesville, VA 22908; [f]Department of Pharmacology and Neuroscience, University of North Texas Health Science Center, Fort Worth, TX 76107; [g]North Texas Eye Research Institute, University of North Texas Health Science Center, Fort Worth, TX 76107; [h]Pittsburgh Heart, Lung and Blood Vascular Medicine Institute, University of Pittsburgh, Pittsburgh, PA 15213; [i]Division of Pulmonary, Allergy, and Critical Care Medicine, University of Pittsburgh, Pittsburgh, PA 15213; [j]Department of Medicine, University of Pittsburgh, Pittsburgh, PA 15213; [k]Department of Bioengineering, University of Pittsburgh, Pittsburgh, PA 15213; [l]Department of Molecular Physiology and Biological Physics, University of Virginia, Charlottesville, VA 22908; [m]Department of Anesthesiology, University of Illinois at Chicago, Chicago, IL 60612; and [n]Department of Pharmacology, University of Illinois at Chicago, Chicago, IL 60612

Edited by Richard W. Aldrich, The University of Texas at Austin, Austin, TX, and approved March 15, 2021 (received for review November 13, 2020)

Recent studies have focused on the contribution of capillary endothelial TRPV4 channels to pulmonary pathologies, including lung edema and lung injury. However, in pulmonary hypertension (PH), small pulmonary arteries are the focus of the pathology, and endothelial TRPV4 channels in this crucial anatomy remain unexplored in PH. Here, we provide evidence that TRPV4 channels in endothelial cell caveolae maintain a low pulmonary arterial pressure under normal conditions. Moreover, the activity of caveolar TRPV4 channels is impaired in pulmonary arteries from mouse models of PH and PH patients. In PH, up-regulation of iNOS and NOX1 enzymes at endothelial cell caveolae results in the formation of the oxidant molecule peroxynitrite. Peroxynitrite, in turn, targets the structural protein caveolin-1 to reduce the activity of TRPV4 channels. These results suggest that endothelial caveolin-1–TRPV4 channel signaling lowers pulmonary arterial pressure, and impairment of endothelial caveolin-1–TRPV4 channel signaling contributes to elevated pulmonary arterial pressure in PH. Thus, inhibiting NOX1 or iNOS activity, or lowering endothelial peroxynitrite levels, may represent strategies for restoring vasodilation and pulmonary arterial pressure in PH.

endothelium | pulmonary hypertension | TRP channel | caveolin | peroxynitrite

Pulmonary hypertension (PH) is a degenerative disease characterized by increased pulmonary arterial pressure (PAP) (1). Current therapeutic options for PH patients are aimed at dilating pulmonary arteries (PAs) to lower PAP. However, treatments that target the mechanisms for impaired vasodilation are not available. Endothelial cells (ECs) promote vasodilation of PAs under normal conditions. Loss of endothelium-dependent vasodilation of resistance-sized PAs is a significant contributor to elevated PAP in PH (2). Therefore, a detailed understanding of the pathological signatures of arterial ECs is necessary for designing therapeutic options capable of rescuing endothelium-dependent vasodilation in PH.

Intracellular Ca^{2+} is an essential regulator of EC function in the pulmonary circulation. Recent studies show that Ca^{2+} influx through EC transient receptor potential vanilloid 4 ($TRPV4_{EC}$) channels dilates resistance PAs via activation of endothelial nitric oxide synthase (eNOS) (3, 4). However, the physiological role of $TRPV4_{EC}$ channels in regulating PAP remains unknown, largely due to the lack of studies in cell-specific knockout mice. In this regard, activation of smooth muscle cell TRPV4 ($TRPV4_{SMC}$) channels can induce PA constriction (5), whereas activation of $TRPV4_{EC}$ channels induces PA dilation (4). We hypothesized that $TRPV4_{EC}$ channel dysfunction contributes to the loss of vasodilation and elevation of PAP in PH.

Caveolin-1 (Cav-1) is an important scaffolding protein that interacts with and stabilizes several other proteins in the pulmonary circulation, including eNOS (6). Global Cav-$1^{-/-}$ mice show elevated PAP, and endothelial Cav-1 (Cav-1_{EC})–dependent signaling is altered in PH (7–11). Studies on pulmonary EC culture showed that the $TRPV4_{EC}$ channel coimmunoprecipitates with Cav-1 (12); however, direct functional evidence for the effect of Cav-1 on $TRPV4_{EC}$ channel activity is lacking. We postulated that Cav-1_{EC} enhances $TRPV4_{EC}$ channel activity in PAs and that impaired Cav-1_{EC}–$TRPV4_{EC}$ signaling contributes to the loss of vasodilation and elevated PAP in PH.

The generation of reactive oxygen species (ROS) appears to be central to vascular dysfunction in PH (13, 14). In this regard,

Significance

Pulmonary hypertension (PH) is a serious disorder with a mortality rate of 40% over 5 y after diagnosis. Endothelial dysfunction is a major contributor to increased pulmonary arterial pressure (PAP) in PH. Here, we provide evidence that endothelial cell caveolin-1–TRPV4 channel signaling lowers resting PAP. Moreover, an impairment of endothelial caveolin-1–TRPV4 channel signaling elevates PAP in PH. In PH, there is an up-regulation of NOX1 and iNOS enzymes in endothelial cells, which increases peroxynitrite levels. Peroxynitrite, in turn, targets endothelial caveolin-1 and lowers endothelial caveolin-1–TRPV4 channel signaling. Finally, decreasing peroxynitrite levels rescues endothelial caveolin-1–TRPV4 channel signaling and lowers PAP in PH.

Author contributions: S.K.S. designed research; Z.D., C.M., M.O., Y.-L.C., T.M.B., M.K., A.Z., H.Q.T., R.B.K., V.E.L., and S.K.S. performed research; A.D.M., Y.S., B.E.I., R.D.M., E.A.G., and S.K.S. contributed new reagents/analytic tools; Z.D., C.M., M.O., Y.-L.C., M.K., A.Z., H.Q.T., C.E.R., R.B.K., G.S.Z., V.E.L., and S.K.S. analyzed data; and Z.D. and S.K.S. wrote the paper.

The authors declare no competing interest.

This article is a PNAS Direct Submission.

[1]To whom correspondence may be addressed. Email: swapnil.sonkusare@virginia.edu.

This article contains supporting information online at https://www.pnas.org/lookup/suppl/doi:10.1073/pnas.2023130118/-/DCSupplemental.

Published April 20, 2021.

NADPH oxidase 1 (NOX1) has emerged as a crucial source of endothelial superoxide radicals in PH (15–17). Interestingly, superoxide radicals were shown to augment TRPV4 channel-induced increases in global Ca^{2+} in pulmonary EC culture (18). Additionally, superoxide radicals can quickly react with NO to form the oxidant molecule peroxynitrite (PN) (19). PN is elevated in the lungs of PH patients (20) and is known to have deleterious effects on EC function (21). Importantly, inducible NOS (iNOS), which generates NO, is also up-regulated in mouse models of PH and in PH patients (22, 23). Therefore, we hypothesized that NOX1 and iNOS contribute to ROS-dependent inhibition of Cav-1_{EC}–$TRPV4_{EC}$ channel signaling in PH.

In the current study, we used inducible, EC-specific TRPV4 channel knockout ($TRPV4_{EC}^{-/-}$) and endothelium-specific Cav-1–knockout ($Cav\text{-}1_{EC}^{-/-}$) mice to confirm a vital role for Cav-1_{EC}–$TRPV4_{EC}$ signaling in lowering resting PAP. Cav-1_{EC}–$TRPV4_{EC}$

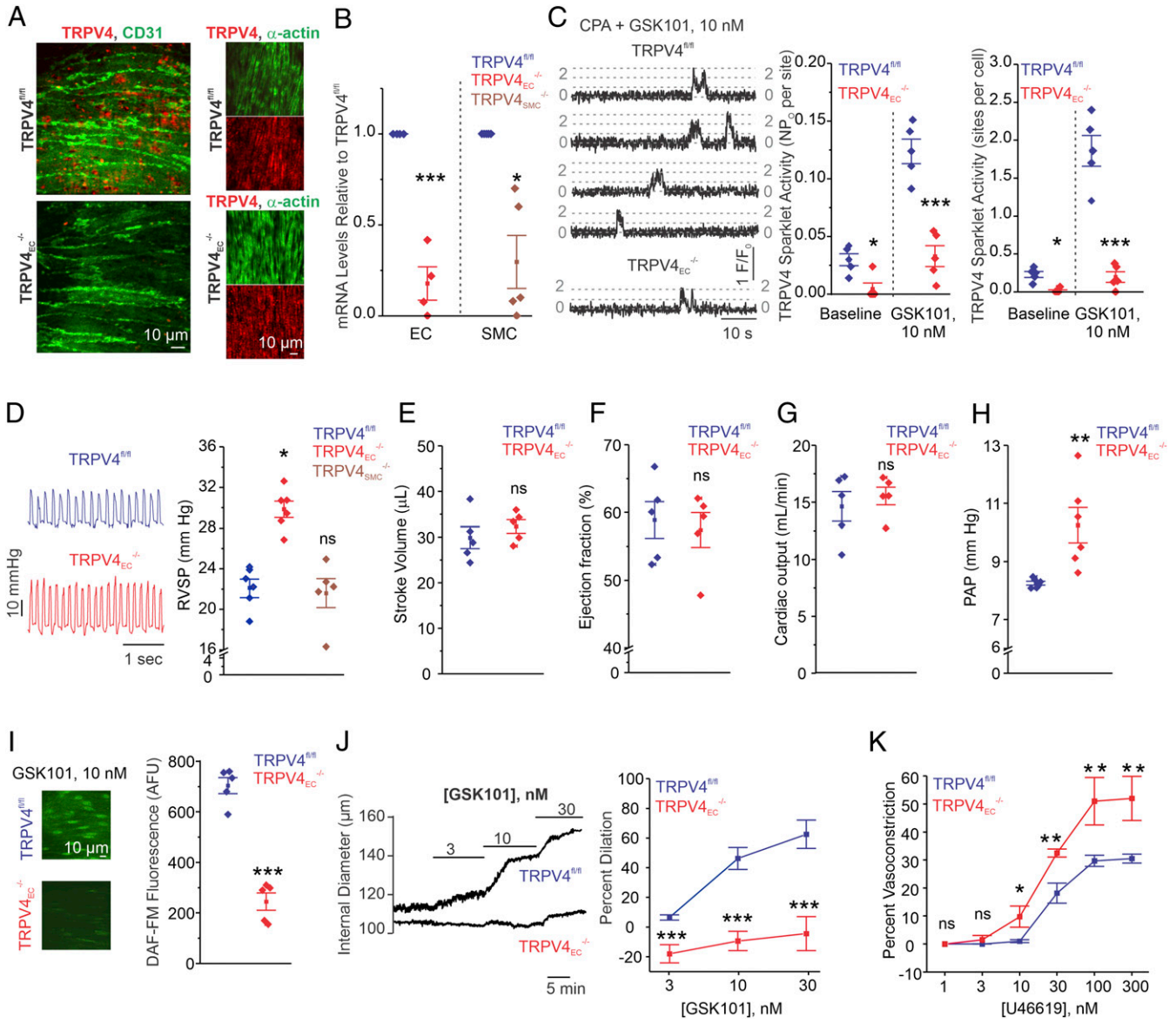

Fig. 1. Inducible $TRPV4_{EC}^{-/-}$ mice show elevated resting PAP. (*A*) $TRPV4_{EC}$ immunofluorescence images in en face fourth-order PAs from $TRPV4^{fl/fl}$ and $TRPV4_{EC}^{-/-}$ mice. (*B*) Endothelial TRPV4 mRNA levels (left of the dotted line) relative to those in $TRPV4^{fl/fl}$ mice and SMC TRPV4 mRNA levels (right of the dotted line) relative to those in $TRPV4^{fl/fl}$ mice ($n = 4$ to 5; $^*P < 0.05$, $^{***}P < 0.001$ versus $TRPV4^{fl/fl}$; one-way ANOVA). (*C*, *Left*) $TRPV4_{EC}$ sparklet traces in one EC from a fluo-4–loaded en face PA in response to TRPV4 channel activator GSK101 (10 nmol/L). (*Center*) $TRPV4_{EC}$ sparklet activity in PAs, expressed as NP_O per site ($n = 5$; $^*P < 0.05$; $^{***}P < 0.001$ versus $TRPV4^{fl/fl}$; two-way ANOVA). N is the number of channels per site, and P_O is the open state probability of the channel. Experiments were performed in Fluo-4–loaded fourth-order PAs in the presence of cyclopiazonic acid (CPA; 20 μmol/L) to eliminate Ca^{2+} release from intracellular stores. (*Right*) $TRPV4_{EC}$ sparklet activity sites per cell in PAs ($n = 5$; $^*P < 0.05$; $^{***}P < 0.001$ versus $TRPV4^{fl/fl}$; two-way ANOVA). (*D*) Representative RVSP (millimeters of mercury) traces (*Left*) and averaged RVSP values (*Right*; $n = 6$; $^*P < 0.05$ versus $TRPV4^{fl/fl}$; ns indicates no significance; one-way ANOVA). (*E*) Averaged stroke volume (microliters) in $TRPV4^{fl/fl}$ and $TRPV4_{EC}^{-/-}$ mice. Data represented as mean ± SEM ($n = 5$). (*F*) Averaged ejection fraction (%) in $TRPV4^{fl/fl}$ and $TRPV4_{EC}^{-/-}$ mice ($n = 5$ mice; ns indicates no significance). (*G*) Cardiac output (milliliters per minute) in $TRPV4^{fl/fl}$ and $TRPV4_{EC}^{-/-}$ mice ($n = 5$ mice). (*H*) Averaged PAP (mm Hg) in isolated perfused lungs from $TRPV4^{fl/fl}$ and $TRPV4_{EC}^{-/-}$ mice ($n = 6$; $^{**}P < 0.01$; *t* test). (*I*) DAF-FM fluorescence analysis of NO production in response to GSK101 (10 nmol/L) in $TRPV4^{fl/fl}$ and $TRPV4_{EC}^{-/-}$ mice, respectively ($n = 5$; $^{***}P < 0.001$; *t* test). (*J*) Pressure myography traces (*Left*) and averaged percent vasodilation (*Right*) of PAs to GSK101 (3 to 30 nmol/L). Fourth-order PAs were pressurized to 15 mm Hg ($n = 5$ to 6; $^{***}P < 0.001$ versus $TRPV4^{fl/fl}$; two-way ANOVA). (*K*) Percent vasoconstriction of PAs in response to the thromboxane A2 receptor agonist U46619 (1 to 300 nmol/L; $n = 5$; $^*P < 0.05$ [10 nmol/L] and $^{**}P < 0.01$ [30 to 300 nmol/L] versus $TRPV4^{fl/fl}$, two-way ANOVA).

signaling was impaired in resistance PAs from mouse models of PH and those from pulmonary arterial hypertension (PAH) patients. NADPH oxidase enzyme 1 ($NOX1^{-/-}$) and inducible nitric oxide synthase ($iNOS^{-/-}$) mice were protected against the impairment of Cav-1_{EC}–$TRPV4_{EC}$ signaling in PH, and NOX1/iNOS/PN inhibitors rescued Cav-1_{EC}–$TRPV4_{EC}$ signaling in PH. Collectively, our findings provide evidence that pathological signaling made possible by the colocalization of NOX1 and iNOS with Cav-1 underlies the loss of $TRPV4_{EC}$ channel activity and vasodilation in PH. Therefore, inhibiting NOX1/iNOS or suppressing PN formation may be a viable strategy for rescuing endothelial function and PAP in PH.

Results

Endothelial, but Not Smooth Muscle, TRPV4 Channels Control Resting PAP. To determine the physiological role of $TRPV4_{EC}$ channels, we utilized inducible $TRPV4_{EC}^{-/-}$ mice. Endothelial knockout of TRPV4 channels was confirmed at the protein level by immunofluorescence analysis of en face PA preparations (Fig. 1*A*) and at the mRNA level by RT-qPCR analysis of ECs from resistance-sized, fourth-order PAs (~50 μm, Fig. 1*B*). Localized, unitary Ca^{2+} influx events through $TRPV4_{EC}$ channels, termed $TRPV4_{EC}$ sparklets (24), were recorded in en face PAs loaded with Fluo-4. Baseline $TRPV4_{EC}$ sparklet activity and activity induced by the specific TRPV4 channel agonist, GSK1016790A (10 nmol/L; hereafter, GSK101), were significantly reduced in PAs from $TRPV4_{EC}^{-/-}$ mice compared with those in PAs from $TRPV4^{fl/fl}$ control mice (tamoxifen-injected $TRPV4^{fl/fl}$ Cre^{-}; Fig. 1*C*). Thus, we can significantly reduce $TRPV4_{EC}$ channel expression and function specifically in the endothelium.

The functional effect of $TRPV4_{EC}^{-/-}$ was determined using right ventricular systolic pressure (RVSP) and PAP measurements, functional magnetic resonance imaging (MRI) analyses, and pressure myography studies in PAs. $TRPV4_{EC}^{-/-}$ mice, but not $TRPV4_{SMC}^{-/-}$ mice, exhibited elevated RVSP, an indirect indicator of PAP (Fig. 1*D*). To ensure that changes in RVSP were not influenced by altered cardiac function, we performed functional MRI analyses on $TRPV4^{fl/fl}$ and $TRPV4_{EC}^{-/-}$ mice. The two genotypes showed no significant differences in heart rate, stroke volume, ejection fraction, and cardiac output (Fig. 1 *E*–*G* and *SI Appendix*, Table S1). Furthermore, isolated lung perfusion experiments showed that PAP was elevated in $TRPV4_{EC}^{-/-}$ mice when compared with $TRPV4^{fl/fl}$ mice (Fig. 1*H*). Fulton index, a ratio of right ventricular (RV) weight to left ventricle and septal (LV+S) weight, was not altered in $TRPV4_{EC}^{-/-}$ mice, suggesting a lack of RV hypertrophy in these mice (*SI Appendix*, Fig. S1).

Consistent with the previously reported $TRPV4_{EC}$–eNOS signaling in PAs (4), GSK101 (10 nmol/L)-induced endothelial NO levels, measured using a fluorescent NO indicator (4-amino-5 methylamino-2′,7′difluorofluorescenin diacetate or DAF-FM, 5 μmol/L), were lower in $TRPV4_{EC}^{-/-}$ mice (Fig. 1*I* and *SI Appendix*, Fig. S2). Reduced $TRPV4_{EC}$ sparklet activity resulted in impaired endothelium-dependent vasodilation to GSK101 (3 to 30 nmol/L) in isolated, pressurized PAs from $TRPV4_{EC}^{-/-}$ mice compared with those from $TRPV4^{fl/fl}$ mice (Fig. 1*J*). Moreover, contractile responses to the thromboxane A_2 receptor agonist U46619 were greater in pressurized PAs from $TRPV4_{EC}^{-/-}$ mice (Fig. 1*K*). Together, these data provide evidence that $TRPV4_{EC}$ channel activity lowers PAP, an effect that is independent of changes in cardiac function.

Cav-1_{EC}–Protein Kinase C Signaling Enhances $TRPV4_{EC}$ Channel Activity and Lowers PAP. Cav-1 was shown to coimmunoprecipitate with TRPV4 channels in pulmonary EC culture (12). However, functional evidence for the effect of Cav-1 on $TRPV4_{EC}$ channel activity is lacking. We hypothesized that Cav-1_{EC} enhances $TRPV4_{EC}$ channel activity in PAs. To determine whether Cav-1_{EC} regulates $TRPV4_{EC}$ channel activity in PAs, we utilized an inducible Cav-$1_{EC}^{-/-}$ mouse. Endothelial Cav-1_{EC} knockout was confirmed by a reduction in Cav-1_{EC} immunostaining (Fig. 2*A*) and Cav-1 messenger RNA (mRNA) levels (Fig. 2*B*). Loss of Cav-1_{EC} resulted in elevated RVSP without RV hypertrophy (Fig. 2 *C*, *Left* and *SI Appendix*, Fig. S1). Isolated lung perfusion experiments showed that PAP was elevated in Cav-$1_{EC}^{-/-}$ mice compared with floxed Cav-1 (Cav-$1^{fl/fl}$) mice (Fig. 2 *C*, *Right*). In PAs from Cav-$1_{EC}^{-/-}$ mice, baseline as well as GSK101-induced $TRPV4_{EC}$ sparklet activity was reduced when compared with the corresponding activities in PAs from Cav-$1^{fl/fl}$ mice, confirming Cav-1_{EC} regulation of $TRPV4_{EC}$ channel activity (Fig. 2 *D* and *E*). At higher levels of activation (GSK101, 30 nmol/L), however, there was no difference in $TRPV4_{EC}$ sparklet activity between the two groups, indicating that Cav-$1_{EC}^{-/-}$ does not reduce the total number of functional $TRPV4_{EC}$ channels per site. GSK101 (10 nmol/L)-induced currents through $TRPV4_{EC}$ channels were reduced in PAs from Cav-$1_{EC}^{-/-}$ mice when compared to the Cav-$1^{fl/fl}$ mice (Fig. 2 *F* and *G*). Higher concentration of the agonist (100 nmol/L), however, elicited similar currents through the $TRPV4_{EC}$ channel (Fig. 2*G*), further supporting unaltered maximum functional $TRPV4_{EC}$ channels in PAs from Cav-$1_{EC}^{-/-}$ and Cav-$1^{fl/fl}$ mice.

Protein kinase C (PKC) is a binding partner of Cav-1 (12) and a well-known activator of $TRPV4_{EC}$ channels (25). HEK293 cells expressing TRPV4 channels + Cav-1 showed higher TRPV4 currents compared to the cells expressing TRPV4 channels alone (Fig. 2*H*). The presence of selective PKC-α/β inhibitor Gö-6976 (1 μmol/L) abolished the difference in TRPV4 currents between TRPV4 and TRPV4 + Cav-1 expressing cells (Fig. 2*H*), supporting the PKC-α/β–dependent nature of Cav-1–TRPV4 channel interaction. Gö-6976 reduced $TRPV4_{EC}$ sparklet activity in Cav-$1^{fl/fl}$ mice but not Cav-$1_{EC}^{-/-}$ mice (Fig. 2*I*), indicating that Cav-1_{EC}–PKC signaling enhances $TRPV4_{EC}$ channel activity in PAs.

$TRPV4_{EC}$ channel-mediated dilation of PAs was substantially attenuated in Cav-$1_{EC}^{-/-}$ mice when compared with that in Cav-$1^{fl/fl}$ mice (Fig. 2*J*). U46619-induced vasoconstriction was also greater in PAs from Cav-$1_{EC}^{-/-}$ mice, confirming that PAs in these mice are more contractile (Fig. 2*K*). These results provide direct evidence that Cav-1_{EC} enhances $TRPV4_{EC}$ channel activity in PAs and lowers PAP.

$TRPV4_{EC}$ Channel Activity Is Impaired in Resistance PAs from Mouse Models of PH and PH Patients. The mechanisms underlying the loss of endothelium-dependent dilation of PAs in PH are poorly understood. We hypothesized that impaired $TRPV4_{EC}$ channel activity contributes to the reduced vasodilation and elevated PAP in PH. $TRPV4_{EC}$ channel activity in resistance PAs was analyzed in two mouse models of PH: chronic hypoxia (CH) and SU5416 (VEGF receptor antagonist) + CH (Su+CH), which is known to cause a more profound PH phenotype than CH alone (26). CH mice showed elevated RVSP and PAP accompanied by RV hypertrophy, indicative of robust development of PH (Fig. 3*A* and *SI Appendix*, Fig. S1). In mice exposed to SU+CH, both RVSP and Fulton index increased to a greater extent than that observed in mice exposed to CH alone, consistent with earlier reports (26). Baseline and GSK101 (10 nmol/L)-induced $TRPV4_{EC}$ sparklet activity was lower in PAs from CH or Su+CH mice compared to PAs from normoxic (N) mice (Fig. 3*B* and *SI Appendix*, Table S2). There was, however, no difference in $TRPV4_{EC}$ sparklet activity among the groups at a higher level of activation (30 nmol/L GSK101; Fig. 3*B*), suggesting that the number of functional $TRPV4_{EC}$ channels is unaltered in PH. Ionic currents through $TRPV4_{EC}$ channels were also decreased in ECs from Su+CH mice when compared with N mice (Fig. 3*C*). At higher levels of TRPV4 channel activation (100 nmol/L GSK101), however, there was no difference in $TRPV4_{EC}$ currents between the groups, suggesting that the maximum number of functional TRPV4 channels is not altered in PH.

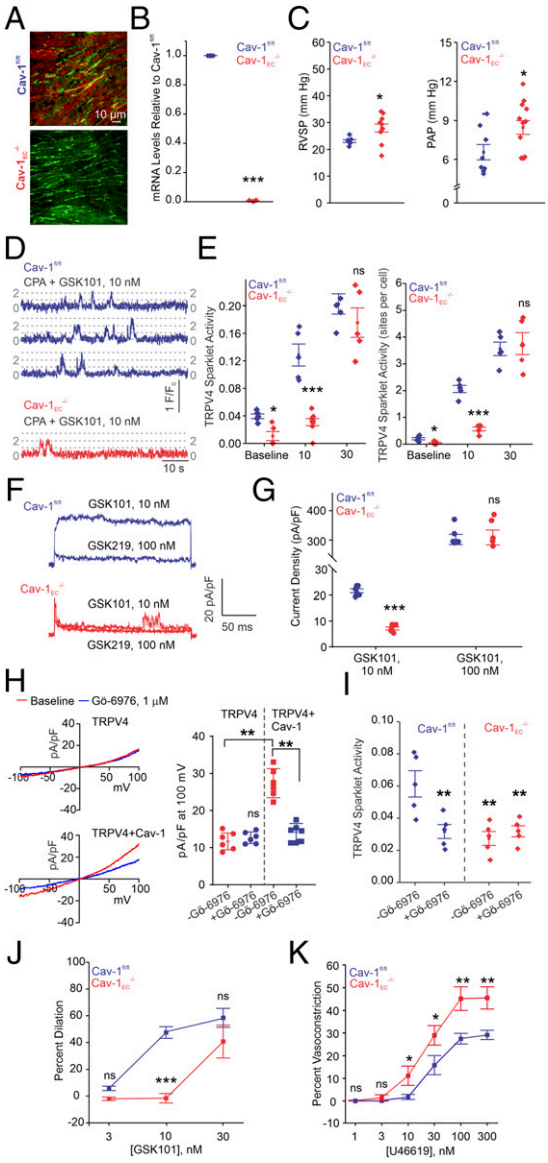

Fig. 2. Cav-1_{EC}–$TRPV4_{EC}$ signaling in PAs lowers resting PAP. (*A*) Cav-1_{EC} immunofluorescence in en face preparations of fourth-order PAs. (*B*) Cav-1_{EC} mRNA levels in PAs relative to those in Cav-$1^{fl/fl}$ mice ($n = 4$; $^{***}P < 0.001$; *t* test). (*C*) Averaged resting RVSP (*Left*; $n = 5$ to 9; $^{*}P < 0.05$; *t* test) and PAP values (*Right*; $n = 8$ to 11; $^{*}P < 0.05$; *t* test). (*D*) $TRPV4_{EC}$ sparklet traces in one EC from a fluo-4–loaded en face PAs in response to TRPV4 channel activator GSK101 (10 nmol/L) in Cav-$1^{fl/fl}$ and Cav-$1_{EC}^{-/-}$ mice. (*E*, *Left*) Baseline or GSK101-induced (10 to 30 nmol/L) $TRPV4_{EC}$ sparklet activity, expressed as NP_O per site ($n = 5$; $^{*}P < 0.05$ versus Cav-$1^{fl/fl}$ [Baseline]; $^{***}P < 0.001$ versus Cav-$1^{fl/fl}$ [10 nmol/L]; ns indicates no significance; two-way ANOVA). Experiments were performed in fluo-4–loaded fourth-order PAs in the presence of cyclopiazonic acid (CPA; 20 μmol/L) to eliminate Ca^{2+} release from intracellular stores. (*Right*) $TRPV4_{EC}$ sparklet sites per cell in PAs from Cav-$1^{fl/fl}$ or Cav-$1_{EC}^{-/-}$ mice ($n = 5$; $^{*}P < 0.05$ versus Cav-$1^{fl/fl}$ [Baseline]; $^{***}P < 0.001$ versus Cav-$1^{fl/fl}$ [10 nmol/L]; two-way ANOVA). (*F*) Representative GSK101 (10 nmol/L)-induced outward $TRPV4_{EC}$ currents in freshly isolated ECs from Cav-$1^{fl/fl}$ or Cav-$1_{EC}^{-/-}$ mice and effect of GSK2193874 (GSK219; 100 nmol/L) in the presence of GSK101 (10 nmol/L). (*G*) Scatterplot showing $TRPV4_{EC}$ currents in the presence of GSK101 (10 and 100 nmol/L; $n = 5$; $^{***}P < 0.001$ versus Cav-$1^{fl/fl}$ [10 nmol/L]; two-way ANOVA). (*H*, *Left*) Representative traces showing TRPV4 currents in the absence or presence of Gö-6976 (PKC-α/β inhibitor; 1 μmol/L) in HEK293 cells transfected with TRPV4 only or cotransfected with TRPV4 plus WT Cav-1, recorded in the whole-cell patch-clamp configuration. (*Right*) Current density plot of TRPV4 currents at +100 mV in the absence or presence of Gö-6976 (1 μmol/L) in HEK293 cells transfected with TRPV4 or TRPV4 + Cav-1 ($n = 5$; $^{**}P < 0.01$ versus TRPV4 [−Gö-6976] and TRPV4 + Cav-1 [−Gö-6976]; two-way ANOVA). (*I*) Effect of Gö-6976 (1 μmol/L) on $TRPV4_{EC}$ sparklet activity in en face preparations of PAs from Cav-$1^{fl/fl}$ and Cav-$1_{EC}^{-/-}$ mice, expressed as NP_O per site ($n = 5$; $^{**}P < 0.01$ versus Cav-$1^{fl/fl}$ [−Gö-6976]; two-way ANOVA). (*J*) Percent dilation of PAs in response to GSK101 (3 to 30 nmol/L; $n = 6$; $^{***}P < 0.001$ versus Cav-$1^{fl/fl}$ [10 nmol/L]; two-way ANOVA). (*K*) Percent constriction of PAs in response to the thromboxane A2 receptor agonist U46619 (1 to 300 nmol/L; $n = 5$; $^{*}P < 0.05$ versus Cav-$1^{fl/fl}$ [10 and 30 nmol/L]; $^{**}P < 0.01$ versus Cav-$1^{fl/fl}$ [100 and 300 nmol/L]; two-way ANOVA).

Adenosine triphosphate (ATP), an endogenous purinergic receptor agonist, causes endothelium-dependent dilation of PAs through $TRPV4_{EC}$ channel activation (4). ATP-induced activation of $TRPV4_{EC}$ channels was impaired in PAs from mouse models of PH and PAH patients (*SI Appendix*, Fig. S3*A*). Furthermore, ATP-induced dilation of PAs was abolished in Su+CH mice (Fig. 3*D*). Consistent with lower $TRPV4_{EC}$ channel activity, PAs from CH and Su+CH mice showed reduced vasodilation and higher contractility (Fig. 3 *E* and *F*). $TRPV4_{EC}$, Cav-1_{EC}, and PKC mRNA levels were not different between N and Su+CH mice (*SI Appendix*, Fig. S4), further supporting impaired channel regulation instead of altered channel expression in PH.

$TRPV4_{EC}$ channels dilate PAs predominantly through eNOS activation (4). To test whether the reduced $TRPV4_{EC}$ channel-induced vasodilation in mouse models of PH is due to an impaired $TRPV4_{EC}$–eNOS signaling linkage, we measured NO levels using DAF-FM. GSK101 (10 nmol/L)-induced endothelial NO levels were lower in PAs from Su+CH mice compared to the N mice (Fig. 3*G*). Notably, the GSK101 concentration that induced similar levels of $TRPV4_{EC}$ sparklet activation in PAs from N and Su+CH mice (30 nmol/L) produced comparable increases in DAF-FM fluorescence (Fig. 3*G*), indicating that activation of eNOS by $TRPV4_{EC}$ channels is not altered in PH. Furthermore, the NO donor, NONOate (0.1 to 10 μmol/L), was able to dilate PAs from N and CH mice to a similar extent (Fig. 3*H*), indicating that the signaling cascade downstream of NO is not altered in PH and that the impairment in endothelial signaling in PH occurs upstream of eNOS.

Support for the clinical relevance of our findings was provided by assessing $TRPV4_{EC}$ sparklet activity in resistance PAs (~50 μm diameter) from patients of PAH (mean PAP > 25). Compared with the PAs from control individuals, PAs from PAH patients showed a significantly lower $TRPV4_{EC}$ sparklet activity (Fig. 3*I* and *SI Appendix*, Table S2). ATP activation of $TRPV4_{EC}$ sparklets was also impaired in PAs from PAH patients (*SI Appendix*, Fig. S3*B*). Moreover, $TRPV4_{EC}$ channel-induced dilation of PAs was significantly diminished in PAH patients compared with that in control individuals (Fig. 3*J*).

NOX1- and iNOS-Mediated PN Impairs $TRPV4_{EC}$ Channel Activity in PH. Elevated production of superoxide radicals ($O_2\bullet^-$) has been implicated in the pathogenesis of PH (18, 27). In support of this concept, the $O_2\bullet^-$-lowering compound, tempol, rescued $TRPV4_{EC}$ channel activity in Su+CH mice (*SI Appendix*, Fig. S5*A*). We then tested the effects of inhibiting three major sources of $O_2\bullet^-$ formation: NOX1 (NoxA1ds; 1 μmol/L), NOX2 (gp91ds-tat; 1 μmol/L), and mitochondria (mitoQ, 1 μmol/L; Fig. 4 *A*–*C* and *SI Appendix*, Table S3). Only NOX1 inhibition with NoxA1ds rescued $TRPV4_{EC}$ sparklet activity in the two mouse models of PH. qPCR studies showed that endothelial NOX1 mRNA levels were elevated in PAs from Su+CH mice (Fig. 4*D*). Importantly, the increase in RVSP observed in $NOX1^{-/-}$ mice exposed to Su+CH was diminished compared with that in wild-type (WT) Su+CH mice (Fig. 4*E* and *SI Appendix*, Fig. S6). Moreover, $NOX1^{-/-}$ mice exposed to Su+CH showed no impairment in $TRPV4_{EC}$ sparklet activity (Fig. 4*F*) or vasodilation (Fig. 4*G*), confirming an important role for endothelial NOX1-derived $O_2\bullet^-$ in reducing $TRPV4_{EC}$ channel activity

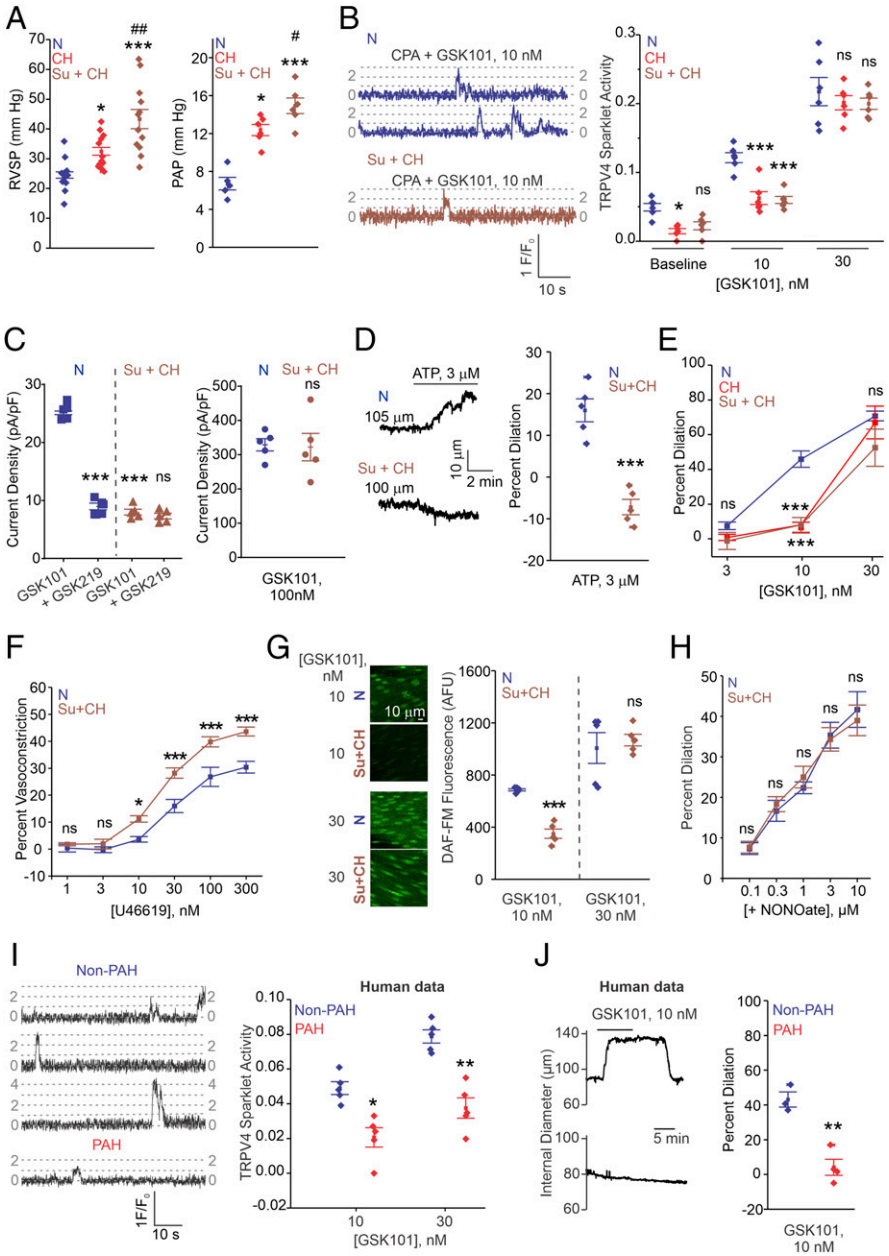

Fig. 3. $TRPV4_{EC}$ channel activity and vasodilation are reduced in PAs from mouse models of PH and PAH patients. (*A*, *Left*) Averaged RVSP (mmHg) values in mice exposed to N, CH (3 wk; 10% O_2), or Su+CH (n = 12; $^{*}P < 0.05$ versus N; $^{***}P < 0.001$ versus N; $^{\#\#}P < 0.01$ versus CH; one-way ANOVA). (*Right*) Averaged PAP (millimeters of mercury) values in mice exposed to N, CH, and Su+CH (n = 6; $^{*}P < 0.05$ versus N; $^{***}P < 0.001$ versus N; $^{\#}P < 0.05$ versus CH; one-way ANOVA). (*B*, *Left*) $TRPV4_{EC}$ sparklet traces in one EC from a fluo-4–loaded en face PA from N and Su+CH mice in response to TRPV4 channel activator GSK101 (10 nmol/L). (*Right*) Baseline or GSK101 (10 and 30 nmol/L)-induced $TRPV4_{EC}$ sparklet activity in N, CH, or Su+CH mice, expressed as NP_O per site (n = 5; $^{*}P < 0.05$ versus N [baseline]; $^{***}P < 0.001$ versus N [10 nmol/L]; two-way ANOVA). Experiments were performed in fluo-4–loaded fourth-order PAs in the presence of cyclopiazonic acid (CPA; 20 μmol/L) to eliminate Ca^{2+} release from intracellular stores. (*C*, *Left*) GSK101 (10 nmol/L)-induced outward currents at +100 mV and inhibition by GSK2193874 (GSK219; 100 nmol/L; n = 5; $^{***}P < 0.001$ versus N [GSK101]; two-way ANOVA). (*Right*) GSK101 (100 nmol/L)-induced outward currents at +100 mV in PAs from N and Su+CH mice (n = 5). (*D*) Pressure myography trace (*Left*) and percent vasodilation (*Right*) of PAs in response to ATP (3 μmol/L) in N and Su+CH mice (n = 5; $^{***}P < 0.001$ versus N; t test). (*E*) Percent vasodilation of PAs from N, CH, and Su+CH mice in response to GSK101 (3 to 30 nmol/L; n = 5 to 10; $^{***}P < 0.001$ versus N [GSK101; 10 nmol/L]; two-way ANOVA). (*F*) Percent vasoconstriction to thromboxane A2 receptor agonist U46619 (1 to 300 nmol/L) in PAs from N or Su+CH mice (n = 5; $^{*}P < 0.05$ [U46619; 10 nmol/L] and $^{***}P < 0.001$ [U466; 30 to 300 nmol/L] versus N; two-way ANOVA). (*G*) DAF-FM fluorescence analysis of NO production in response to GSK101 (10 and 30 nmol/L) in N and Su+CH mice, respectively (n = 5; $^{***}P < 0.001$ versus N [GSK101; 10 nmol/L]; two-way ANOVA). (*H*) Percent vasodilation of PAs from N and Su+CH mice in response to spermine NONOate (NO donor; 0.1 to 10 μmol/L; n = 5). (*I*) $TRPV4_{EC}$ sparklet traces (*Left*) and GSK101 (10 and 30 nmol/L)-induced sparklet activity (*Right*) in PAs from non-PAH and PAH patients (n = 5; $^{*}P < 0.05$ [GSK101; 10 nmol/L] versus non-PAH; $^{**}P < 0.01$ [GSK101; 30 nmol/L] versus non-PAH; two-way ANOVA). (*J*, *Left*) Representative diameter traces showing GSK101 (10 nmol/L)-induced dilation of PAs from non-PAH individuals and PAH patients, preconstricted with U46619 (50 nmol/L). (*Right*) Percent vasodilation of PAs from non-PAH and PAH patients in response to GSK101 (10 nmol/L; n = 3 to 4; $^{**}P < 0.01$; t test).

in PH. However, excessive generation of $O_2\bullet^-$ using a hypoxanthine/xanthine oxidase system did not alter $TRPV4_{EC}$ channel activity in normal PAs, supporting the concept that $O_2\bullet^-$ by itself does not inhibit $TRPV4_{EC}$ channel activity in PAs (*SI Appendix*, Fig. S5*B*). Hypoxanthine/xanthine oxidase can also increase the production of hydrogen peroxide. In this regard, we previously demonstrated that hydrogen peroxide does not directly alter $TRPV4_{EC}$ sparklet activity (21). We therefore explored the possibility that $O_2\bullet^-$ reacts with NO, the predominant signaling molecule in the pulmonary circulation, to form the oxidant molecule PN.

Pulmonary PN levels are elevated in PH (20, 28), and PN was shown to have detrimental effects on $TRPV4_{EC}$ channel activity and endothelial function in obesity (21). Measurement of PN levels using the fluorescent indicator, coumarin boronic acid, confirmed higher endothelial PN levels in PAs from mouse models of PH (Fig. 5*A* and *SI Appendix*, Fig. S2). While eNOS activity is impaired in PH (29), iNOS activity has been shown to be elevated (22, 23) and may provide NO for PN formation. The specific iNOS inhibitor 1400W rescued $TRPV4_{EC}$ sparklet activity in Su+CH mice (Fig. 5*B* and *SI Appendix*, Table S3), suggesting that iNOS contributes to PN formation in PH. Endothelial iNOS mRNA levels were elevated in Su+CH mice (Fig. 5*C*). RVSP in $iNOS^{-/-}$ mice exposed to Su+CH was lower than that in WT Su+CH mice (Fig. 5*D* and *SI Appendix*, Fig. S6), but $TRPV4_{EC}$ sparklet activity (Fig. 5*E* and *SI Appendix*, Table S3) and vasodilation (Fig. 5*F*) were not impaired in PAs from $iNOS^{-/-}$ mice exposed to Su+CH (*SI Appendix*, Fig. S6). Moreover, PN levels in both $iNOS^{-/-}$ and $NOX1^{-/-}$ mice exposed to Su+CH were lower than those in WT Su+CH mice (*SI Appendix*, Fig. S7*A*). Together, these results identify NOX1 and iNOS as the major contributors to endothelial PN formation in PH.

Similar to the results from mouse models, studies in PAs from PAH patients and control individuals showed higher endothelial PN levels in PAH patients (*SI Appendix*, Fig. S7*B*). Moreover, $TRPV4_{EC}$ sparklet activity in PAs from PAH patients was rescued

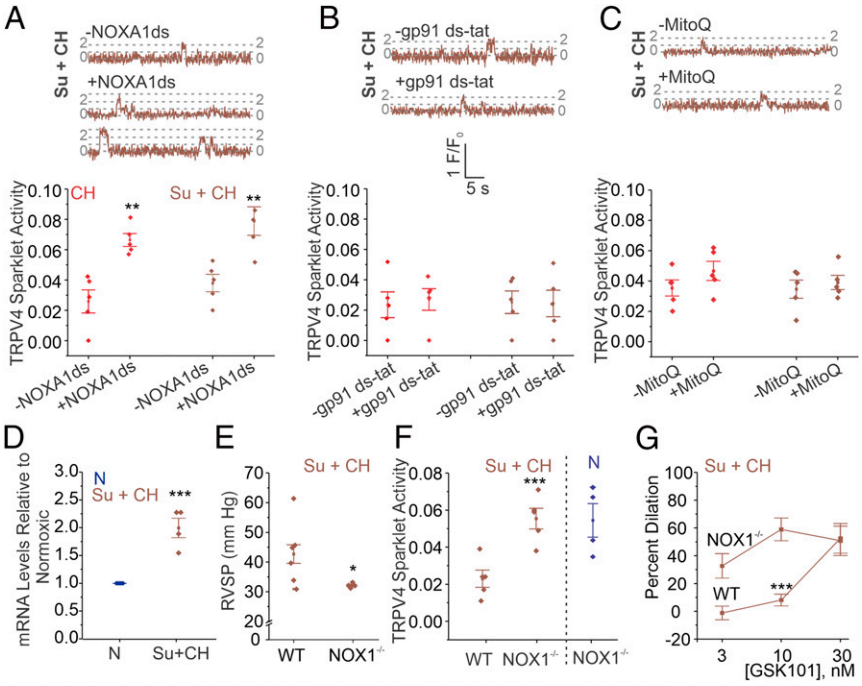

Fig. 4. Endothelial NOX1 impairs $TRPV4_{EC}$ channel activity in PH. (*A*–*C*) $TRPV4_{EC}$ sparklet traces in one EC from a fluo-4–loaded en face PA (*Top*) and $TRPV4_{EC}$ sparklet activity per site (*Bottom*; NP_O per site) in the absence and presence of NOXA1ds (NOX 1 inhibitor; 1 μmol/L; *A*), gp91ds-tat (NOX2 inhibitor; 1 μmol/L; *B*), or mitoQ (mitochondrial antioxidant; 1 μmol/L; *C*) in PAs from C57BL6/J mice exposed to CH (3 wk; 10% O_2) or Su+CH ($n = 5$; $^{**}P < 0.01$ versus [–NOXA1ds]; two-way ANOVA), expressed as NP_O per site. (*D*) NOX1 mRNA levels in ECs from N and Su+CH mice relative to N mice ($n = 5$; $^{***}P < 0.001$; *t* test). (*E*) Averaged resting RVSP (millimeters of mercury) values in WT and $NOX1^{-/-}$ mice exposed to Su+CH ($n = 4$ to 6; $^{*}P < 0.05$; *t* test). (*F*) GSK101-induced (1 nmol/L) $TRPV4_{EC}$ sparklet activity in PAs from WT and $NOX1^{-/-}$ mice exposed to Su+CH and $NOX1^{-/-}$ mice exposed to N ($n = 5$; $^{***}P < 0.001$ versus WT [Su+CH]; two-way ANOVA). (*G*) Percent dilation of PAs from WT and $NOX1^{-/-}$ mice exposed to Su+CH in response to GSK101 (3 to 30 nmol/L; $n = 5$; $^{***}P < 0.001$ versus WT [3 and 10 nmol/L]; two-way ANOVA).

by inhibitors of iNOS or NOX1 (Fig. 5 *G* and *H* and *SI Appendix*, Table S3). These findings demonstrate that iNOS and NOX1 contribute to PN formation and impaired $TRPV4_{EC}$ channel activity in clinical PAH.

PN Targets Cav-1_{EC} to Lower Cav-1_{EC}–$TRPV4_{EC}$ Channel Signaling in PH. Specific PN inhibitors are not available; therefore, we used three different compounds that are known to lower PN levels: PN scavengers uric acid (UA; 200 μmol/L; Fig. 6*A*) and ebselen (1 μmol/L) and PN decomposer Fe^{III}-tetra-(4-sulfonatophenyl)-porphyrin (FeTPPS; 1 μmol/L; *SI Appendix*, Fig. S8 *A* and *B*). All three compounds rescued $TRPV4_{EC}$ sparklet activity in PAs from mouse models of PH. PEG-catalase (500 U/mL), which breaks down H_2O_2, or taurine (1 mmol/L), which decreases hypochlorous acid levels, had no effect on $TRPV4_{EC}$ sparklet activity in PH (*SI Appendix*, Fig. S8 *C* and *D*), indicating that neither H_2O_2 nor hypochlorous acid are responsible for reducing $TRPV4_{EC}$ channel activity in PH. PN inhibition also rescued $TRPV4_{EC}$ channel-induced vasodilation in Su+CH mice (*SI Appendix*, Fig. S9 and Table S3). Strikingly, acute treatment with FeTPPS (30 mg/kg, intraperitoneally [i.p.]) reduced the RVSP of CH mice to normal levels but had no effect on RVSP in N mice (Fig. 6*B*). UA (200 μmol/L) also increased the activity of $TRPV4_{EC}$ channels and $TRPV4_{EC}$ channel-mediated vasodilation in PAs from PAH patients, indicating a clinically relevant role of PN formation in impairing $TRPV4_{EC}$ channel activity in PH (Fig. 6 *C* and *D*). Importantly, while UA was able to rescue $TRPV4_{EC}$ sparklet activity and vasodilation in PAs from WT mice exposed to Su+CH (Fig. 6*A* and *SI Appendix*, Fig. S9), it was unable to rescue $TRPV4_{EC}$ sparklet activity or vasodilation in Cav-$1_{EC}^{-/-}$ mice exposed to Su+CH (Fig. 6 *E* and *F*), suggesting that PN may be targeting Cav-1_{EC} to impair $TRPV4_{EC}$ channel activity.

To confirm the inhibitory effect of exogenous PN on $TRPV4_{EC}$ channel activity, we recorded $TRPV4_{EC}$ currents from freshly isolated pulmonary ECs and $TRPV4_{EC}$ sparklet activity in en face PAs. The addition of exogenous PN (5 μmol/L) attenuated $TRPV4_{EC}$ channel currents (*SI Appendix*, Fig. S10*A*) and decreased $TRPV4_{EC}$ sparklet activity (Fig. 7*A*). PN also decreased $TRPV4_{EC}$ channel-induced vasodilation (*SI Appendix*, Fig. S10*B*) but did not affect vasodilation induced by the NO donor, spermine NONOate (*SI Appendix*, Fig. S10*C*), suggesting that PN does not alter signaling elements downstream of NO. Importantly, PN inhibition of $TRPV4_{EC}$ channel activity was absent in PAs from Cav$1_{EC}^{-/-}$ mice (Fig. 7*A*), further supporting the idea that PN may be acting on Cav-1_{EC}, rather than $TRPV4_{EC}$ channels, to lower Cav-1_{EC}–$TRPV4_{EC}$ signaling. The Cav-1_{EC}–dependent nature of PN inhibition of $TRPV4_{EC}$ channels was further confirmed by studies in HEK293 cells expressing TRPV4 channels alone or coexpressing TRPV4 channels and Cav-1 (Fig. 7*B*). PN was only able to inhibit TRPV4 channel currents in the presence of Cav-1, supporting the specificity of PN effects on Cav-1 (Fig. 7*C*). Collectively, these results show that the PN-dependent impairment of Cav1_{EC}–$TRPV4_{EC}$ channel signaling contributes to reduced vasodilation and elevated RVSP in PH.

PN Induces Cysteine Modifications on Cav-1 to Lower TRPV4 Channel Activity. PN is known to induce tyrosine nitration and cysteine modification of proteins. Because the observed PN effects were reversible, we postulated that PN causes reversible cysteine modification(s) on Cav-1. To test this, we generated Cav-1 mutants containing Cys-to-Ala substitutions of each of the three cysteine residues on Cav-1 and exogenously expressed them in HEK293 cells (Fig. 7*D*). The Cys133Ala and Cys156Ala mutations inhibited the effect of PN on TRPV4 channel activity, whereas the Cys-to-Ala modification at Cys143 did not (Fig. 7*E*). Taken together, these results suggest that PN targets Cys133 and Cys156 on Cav-1, thereby reducing TRPV4 channel activity and increasing PAP in PH.

NOX1 and iNOS Colocalize with Cav-1_{EC} in PH. Physiological rescue of $TRPV4_{EC}$ channel activity by PN inhibitors in PH-supported impaired channel regulation, rather than channel expression, as a cause of reduced $TRPV4_{EC}$ channel activity. To that end, the nanometer proximity between Cav-1_{EC} and $TRPV4_{EC}$ channels, assessed with in situ proximity ligation assays (PLAs), was not affected in PH (*SI Appendix*, Fig. S11). However, the nanometer proximity of Cav-1_{EC} with NOX1 and iNOS was increased in Su+CH mice compared with N mice (Fig. 8 *A* and *B*). These results demonstrate higher colocalization of iNOS and NOX1 with Cav-1_{EC} in PH and suggest that PN generation at caveolae may impair Cav-1_{EC}–$TRPV4_{EC}$ signaling. In HEK293 cells

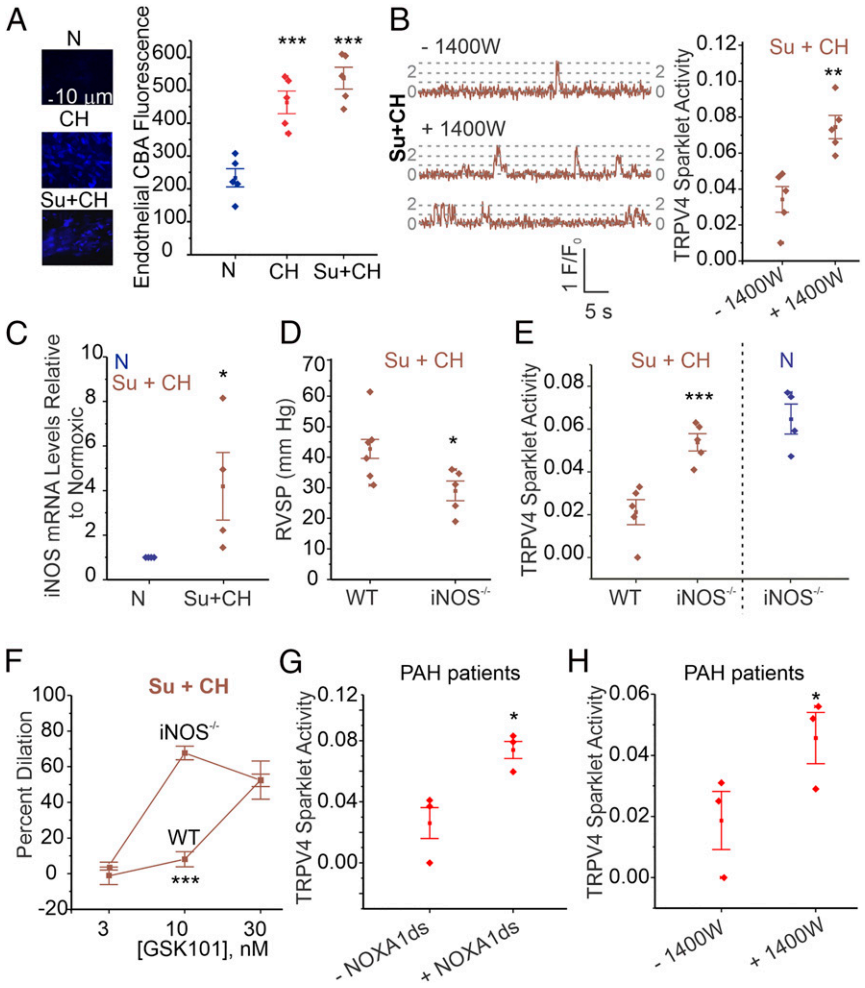

Fig. 5. Endothelial iNOS/NOX1-generated PN impairs $TRPV4_{EC}$ channel activity in PH. (*A*, *Left*) Representative nonconfocal images for coumarin boronic acid (CBA, PN indicator) fluorescence in ECs from PAs of mice exposed to N, CH (3 wk; 10% O_2), or Su+CH. (*Right*) Scatterplot of CBA fluorescence intensity in en face preparations of fourth-order PAs from mice exposed to N, CH, or Su+CH ($n = 5$; $^{***}P < 0.001$ versus N; one-way ANOVA). Experiments were performed in the presence of PEG-catalase (H_2O_2 metabolizing enzyme; 500 U/mL) and taurine (hypochlorous acid-lowering agent; 1 mmol/L). (*B*) $TRPV4_{EC}$ sparklet traces in one EC from fluo-4–loaded en face PAs (*Left*) and sparklet activity per site (*Right*; expressed as NP_O per site) in the absence and presence of the 1400W (iNOS inhibitor; 1 μmol/L) in PAs from C57BL6/J mice exposed to Su+CH ($n = 5$; $^{**}P < 0.01$; *t* test). (*C*) iNOS mRNA levels in ECs from PAs of N and Su+CH mice, expressed relative to N mice ($n = 5$; $^{*}P < 0.05$; *t* test). (*D*) Averaged resting RVSP (millimeters of mercury) values in WT and $iNOS^{-/-}$ mice after exposure to Su+CH ($n = 5$ to 6; $^{*}P < 0.05$; *t* test). (*E*) $TRPV4_{EC}$ sparklet activity in PAs from WT and $iNOS^{-/-}$ mice exposed to Su+CH and $iNOS^{-/-}$ mice exposed to N ($n = 5$; $^{*}P < 0.05$; two-way ANOVA). (*F*) GSK101 (3–30 nmol/L)-induced vasodilation of PAs from WT and $iNOS^{-/-}$ mice exposed to Su+CH ($n = 5$; $^{***}P < 0.001$ versus WT [10 nmol/L]; two-way ANOVA). (*G*) Effect of the NOXA1ds (NOX1 inhibitor, 1 μmol/L) on GSK101 (10 nmol/L)-induced $TRPV4_{EC}$ sparklet activity in PAs from PAH patients ($n = 3$; $^{*}P < 0.05$; *t* test). (*H*) Effect of the 1400W (1 μmol/L) on $TRPV4_{EC}$ sparklet activity in PAs from PAH patients ($n = 3$; $^{*}P < 0.05$; *t* test).

overexpressing Cav-1 with NOX1 or iNOS, Cav-1 coimmunoprecipitated with NOX1 as well as iNOS (*SI Appendix*, Fig. S12), supporting the ability of Cav-1 to associate with iNOS and NOX1.

$Cav\text{-}1_{EC}$ showed nanometer proximity with PKC in PAs from normal mice (Fig. 8*C*). However, in Su+CH mice, the localization of PKC with $Cav\text{-}1_{EC}$ was highly reduced (Fig. 8*C*). PN scavenger UA restored the Cav-1:PKC localization (Fig. 8*C*) and PKC activation of $TRPV4_{EC}$ sparklets in PAs from Su+CH mice (Fig. 8*D*). These results supported the concept that PN-induced cysteine modification on Cav-1 impairs $Cav\text{-}1_{EC}$:PKC localization and $TRPV4_{EC}$ channel activity in PH. The summary of our results is illustrated in Fig. 8*E*.

Discussion

Despite an emerging interest in the contribution of endothelial TRPV4 channels to pulmonary pathologies, including lung edema and lung injury (30–32), the physiological roles of pulmonary $TRPV4_{EC}$ channels remain unknown. Using cell-specific knockout mice, we show that arterial $TRPV4_{EC}$ channels lower resting PAP and that impaired $TRPV4_{EC}$ channel activity contributes to higher PAP in PH. Importantly, data from PAH patients provide evidence that clinical PAH is also associated with the lowering of $TRPV4_{EC}$ channel activity in small PAs. Detailed mechanistic studies show increased association between $Cav\text{-}1_{EC}$ and NOX1/iNOS in PH, resulting in localized PN formation and impaired $Cav\text{-}1_{EC}$–$TRPV4_{EC}$ channel signaling. Overall, our studies identify specific mechanisms that impair the activity of $TRPV4_{EC}$ channels in resistance PAs in PH and lay the foundation for targeting these pathological mechanisms to rescue endothelial function. Recent studies have focused on the detrimental effects of capillary $TRPV4_{EC}$ channels in pulmonary vascular disorders. Indeed, inhibition of TRPV4 channels has been proposed as a treatment option for pulmonary edema (30, 31). Our results indicate that direct TRPV4 channel inhibitor therapy may have undesirable effects on PAP through inhibition of $TRPV4_{EC}$ channels in resistance PAs.

EC and smooth muscle cell (SMC) components in the TRPV4 channel control of PAP have been difficult to define. Global $TRPV4^{-/-}$ mice show no changes in resting RVSP (5). Administration of the TRPV4 channel activator GSK101 was shown to reduce RVSP in rats (33), although the exact cell types involved in this effect were not clear. TRPV4 channels are also detected at mRNA and protein levels in pulmonary vascular SMCs (34). SMC TRPV4 channels promote PA contractility (35) and are upregulated following CH (5, 36). Thus, EC and SMC TRPV4 channels appear to have contrasting effects on contractility, similar to intracellular Ca^{2+} in ECs and SMCs (37). In other words, it appears that EC TRPV4 channels are dilatory, whereas SMC TRPV4 channels are contractile in PAs. These findings further exemplify the unique cellular activation/function of TRPV4 channels in ECs or SMCs, which would be difficult to decipher using global knockout mice. We provide evidence that resting RVSP is not altered in $TRPV4_{SMC}^{-/-}$ mice (Fig. 1*D*), suggesting that SMC TRPV4 channels may not play a role in regulating the resting PAP. The lack of a resting PAP phenotype in global $TRPV4^{-/-}$ mice (5) but elevated PAP in endothelial $TRPV4^{-/-}$

mice are consistent with previously published findings of unaltered resting systemic blood pressure in TRPV4$^{-/-}$ mice (38) and elevated systemic blood pressure in endothelial TRPV4$^{-/-}$ mice (21). Indeed, many global knockout mice are known to have developmental compensations to ensure physiological homeostasis, masking individual cellular function (reviewed in ref. 39). TRPV4 channels have also been reported in alveolar epithelial cells (40), macrophages (41), airway SMCs (42), and epithelial cells (43). Therefore, using direct TRPV4 channel activators to improve vasodilation in PH would likely be associated with multiple side effects. Targeting pathological elements upstream of TRPV4$_{EC}$ channels, namely PN, iNOS, or NOX1, may result in a more specific rescue of TRPV4$_{EC}$ channel activity in resistance PAs in PH.

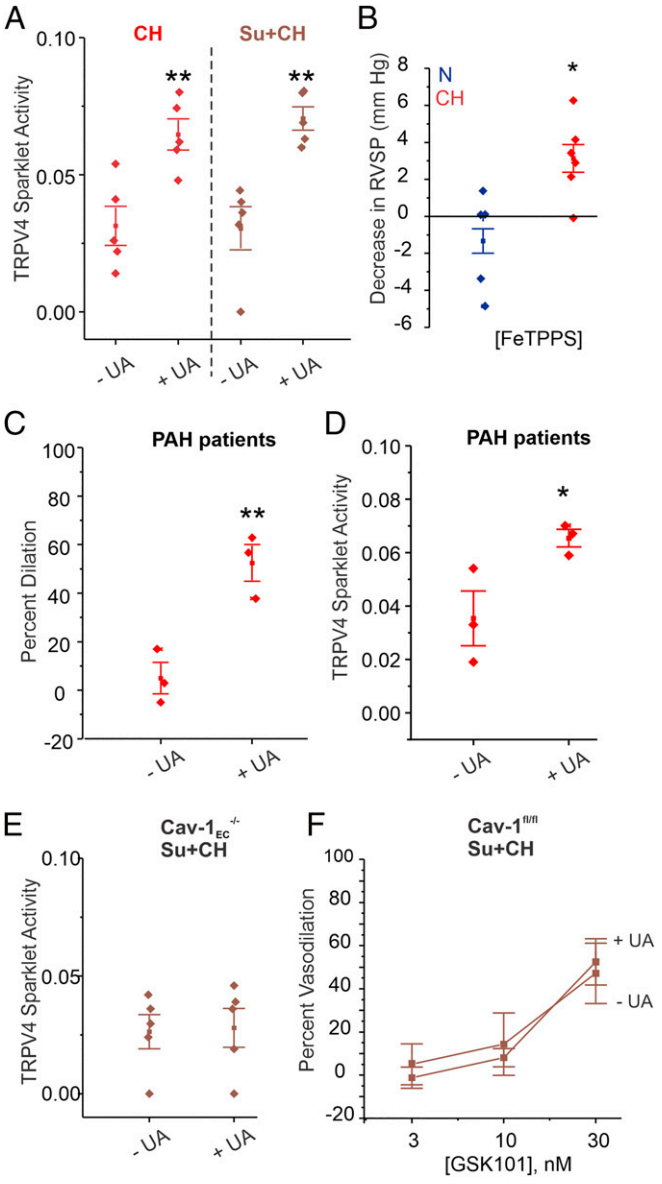

Fig. 6. PN inhibition rescues TRPV4$_{EC}$ channel activity in PH. (*A*) Effects of the UA (PN scavenger; 200 μmol/L) on TRPV4$_{EC}$ sparklet activity in PAs from mice treated with CH (3 wk; 10% O_2) or Su+CH, expressed as NP_O per site ($n = 5$; $^{**}P < 0.01$ versus [–UA]; one-way ANOVA). (*B*) Scatter plot showing the FeTPPS (PN decomposer; 30 mg/kg i.p.)-induced decrease in RVSP (millimeters of mercury) in mice exposed to N or CH ($n = 5$ to 6; $^{*}P < 0.05$; *t* test). (*C*) Effect of UA (200 μmol/L) on GSK101 (10 nmol/L)-induced vasodilation of PAs from PAH patients ($n = 3$; $^{**}P < 0.01$; *t* test). (*D*) Effect of UA (200 μmol/L) on GSK101 (10 nmol/L)-induced TRPV4$_{EC}$ sparklet activity of PAs from PAH patients ($n = 3$; $^{*}P < 0.05$; *t* test). (*E*) Effect of the UA (200 μmol/L) on TRPV4$_{EC}$ sparklet activity in PAs from Cav-1$_{EC}^{-/-}$ mice exposed to Su+CH ($n = 5$). (*F*) Effect of UA (200 μmol/L) on GSK101 (3 to 30 nmol/L)-induced vasodilation of PAs from Cav-1$_{EC}^{-/-}$ mice exposed to Su+CH ($n = 5$).

Endothelial Ca^{2+} has distinct effects on capillary and arterial function. TRPV4$_{EC}$ channel activity in capillary ECs has mostly been associated with detrimental effects in pulmonary pathologies. Excessive capillary TRPV4$_{EC}$ channel activity contributes to increased endothelial permeability (44, 45), lung injury (40), and pulmonary edema (44, 45). A study by Thorneloe et al. (44) showed that chronic treatment with TRPV4 channel inhibitor restored the integrity of the capillary endothelial barrier in heart failure–induced pulmonary edema. However, arterial TRPV4$_{EC}$ channel activity remains an unexplored topic in pulmonary vascular disorders. Our data show that acute treatment with TRPV4 channel inhibitor elevates RVSP, and this effect is lost in TRPV4$_{EC}^{-/-}$ mice (*SI Appendix*, Fig. S13). Capillary and arterial ECs are structurally and functionally heterogeneous (24, 46, 47). Moreover, TRPV4$_{EC}$ channels and Ca^{2+} signaling mechanisms have distinct effects on capillary and arterial function (3, 4, 40, 44). Our data, in conjunction with current evidence in the literature, suggest that pathological conditions may affect capillary and arterial TRPV4$_{EC}$ channels differently.

Pulmonary circulation is a high-flow circulation. Therefore, flow-induced shear stress is a potential activator of TRPV4$_{EC}$ channels in PAs (48–50). Shear stress has also been shown to increase the release of ATP from the pulmonary endothelium (51). Extracellular ATP is a physiological activator of TRPV4$_{EC}$ channels in PAs (4). We show that basal and ATP-induced TRPV4$_{EC}$ channel activity is reduced in PH (Fig. 3*D* and *SI Appendix*, Fig. S3*A*). Therefore, it is possible that flow-induced TRPV4$_{EC}$ channel activation is impaired in PH, which would result in reduced endothelium-dependent vasodilation.

Cav-1$_{EC}$ is a key structural protein in the pulmonary circulation, as demonstrated by the observed increase in RVSP in global Cav-1$^{-/-}$ mice (11, 52). Moreover, Cav-1$_{EC}$–dependent signaling is impaired in PH (7–9). We found that abnormal Cav-1$_{EC}$–TRPV4$_{EC}$ signaling, rather than reduced Cav-1$_{EC}$ or TRPV4$_{EC}$ expression, contributes to endothelial dysfunction in PH. Although qPCR analysis showed a minor decrease in Cav-1$_{EC}$ mRNA levels in PH (*SI Appendix*, Fig. S4), Cav-1$_{EC}$:TRPV4$_{EC}$ localization was not altered in PH. The instantaneous rescue of TRPV4$_{EC}$ channel activity by PN inhibitors also supports the concept that the signaling impairment in PH is not attributable to altered protein expression. Cav-1 is also a well-known anchor protein for eNOS (6), and global Cav-1$^{-/-}$ mice show higher NO and PN levels (52). TRPV4$_{EC}$ channel activity remained low in Cav-1$_{EC}^{-/-}$ mice in the presence of the NOS inhibitor L-NNA (100 μmol/L; *SI Appendix*, Fig. S14), supporting the idea that the decrease in TRPV4$_{EC}$ channel activity in Cav-1$_{EC}^{-/-}$ mice is not due to elevated NO levels.

The spatial proximity of iNOS and NOX1 with Cav-1$_{EC}$ facilitates the formation of endothelial PN in PH. PN is known to have harmful effects on the vascular function in multiple disease conditions. Our previous studies showed that PN targets A-kinase anchoring protein 150 (AKAP150)–TRPV4$_{EC}$ channel signaling in systemic resistance arteries, contributing to systemic hypertension. Notably, AKAP150 is not expressed in PA endothelium. Instead, PN-dependent inhibition of Cav-1$_{EC}$–TRPV4$_{EC}$ channel signaling elevates PAP in PH. Importantly, superoxide radicals do not directly inhibit TRPV4$_{EC}$ channel activity (*SI Appendix*, Fig. S5*B*). In this regard, a previous study on capillary EC culture suggested that superoxide radicals activate TRPV4$_{EC}$ channel-dependent increases in Ca^{2+} (18). TRPV4$_{EC}$ channels promote inositol 1,4,5-trisphosphate (IP_3) receptor (IP_3R)-mediated Ca^{2+} release from the endoplasmic reticulum (ER) (53), and superoxide radicals have been shown to potentiate IP_3Rs (54). Therefore, it

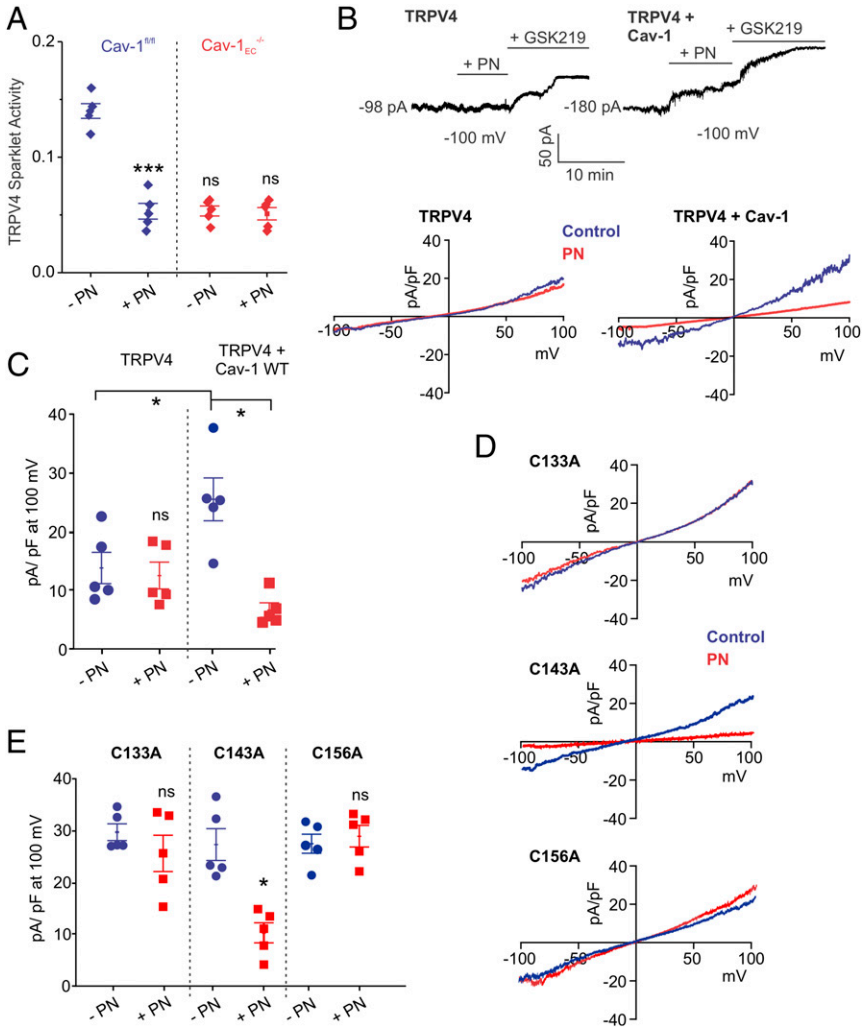

Fig. 7. PN inhibits TRPV4 channel activity by targeting cysteine residues on Cav-1. (*A*) GSK101 (10 nmol/L)-induced $TRPV4_{EC}$ sparklet activity in PAs from Cav-$1^{fl/fl}$ and Cav-$1_{EC}^{-/-}$ mice in the presence or absence of PN (5 μmol/L), expressed as NP_O per site ($n = 5$; ***$P < 0.001$ versus Cav-$1^{fl/fl}$ [−PN]; two-way ANOVA). (*B*, *Top*) Patch-clamp traces showing continuous recordings of TRPV4 currents at −100 mV under basal conditions, followed by PN (5 μmol/L) and GSK2193874 (GSK219; 100 nmol/L) in HEK293 cells transfected with TRPV4 alone or TRPV4 + Cav-1. Cells were held at −100 mV in the whole-cell patch-clamp configuration. (*Bottom*) Representative traces showing TRPV4 currents in the absence or presence of PN (5 μmol/L) in HEK293 cells transfected with TRPV4 alone or TRPV4 + Cav-1, recorded in the whole-cell patch-clamp configuration. (*C*) Current density plot of TRPV4 currents at +100 mV in the absence or presence of PN in HEK293 cells transfected with TRPV4 or TRPV4 + WT Cav-1 ($n = 5$; *$P < 0.05$ versus TRPV4 + Cav-1 [−PN]; two-way ANOVA). (*D*) Representative traces showing TRPV4 currents in the absence or presence of PN in HEK293 cells transfected with TRPV4 plus Cav-1 mutants, recorded in the whole-cell patch-clamp configuration. (*E*) Current density plot of TRPV4 currents at +100 mV in the absence or presence of PN (5 μmol/L) in HEK293 cells transfected with TRPV4 + Cav-1^{C133A}, TRPV4 + Cav-1^{C143A}, or TRPV4 + Cav-1^{C156A} ($n = 5$; * $P < 0.05$ versus [−PN; TRPV4 + Cav-1^{C143A}]; two-way ANOVA).

is possible that superoxide radicals act on IP_3Rs to promote TRPV4–IP_3R-mediated increases in intracellular Ca^{2+}.

iNOS activity has mainly been associated with immune cells (55). The increase in endothelial iNOS mRNA levels (Fig. 5*C*) confirms the up-regulation of endothelial iNOS in PH. However, it should be noted that this increase in iNOS activity did not result in pulmonary vasodilation. We postulate that the reduced bioavailability of NO despite higher iNOS activity is due to the near-instantaneous reaction of NO with NOX1-generated superoxide radicals to form PN. Uncoupling of eNOS has also been proposed as a cause of reduced NO bioavailability in PH (29). However, our results indicate that the $TRPV4_{EC}$–eNOS signaling linkage is not altered in PH (Fig. 3*G*); instead, the signaling abnormalities occur upstream of $TRPV4_{EC}$ channels. PN modification of cysteine residues on Cav-1_{EC} appears to be the mechanism underlying PN-induced impairment of $TRPV4_{EC}$ channel activity. The reversibility of the PN effect on $TRPV4_{EC}$ channel activity implies that PN-induced tyrosine nitration, which is thought to be a permanent modification (56), is unlikely to be the underlying mechanism. The main PN-induced cysteine modifications include disulfide bond formation and S-nitrosylation (56). Previous studies have suggested that Cys156 S-nitrosylation can impair Cav-1–dependent signaling in PAH (7), although identifying which specific type of PN-induced cysteine modification underlies impaired Cav-1_{EC}–$TRPV4_{EC}$ signaling will require further investigation.

The current manuscript presents in vivo RVSP and ex vivo PAP measurements. A significant increase in resting RVSP and PAP within 1 mo of the induction of endothelial knockout is striking. One limitation of the study is that the direct in vivo PAP measurements were not performed. Besides PA contractility, other crucial factors such as blood viscosity may also play a role in regulating PAP and will need to be investigated separately.

In conclusion, arterial Cav-1_{EC}–$TRPV4_{EC}$ channel signaling promotes pulmonary vasodilation, and its impairment contributes to elevated PAP in PH. In PH, up-regulation of NOX1 and iNOS in endothelial caveolae increases PN formation and inhibits the Cav-1_{EC}–$TRPV4_{EC}$ channel signaling linkage. Decreasing PN levels or NOX1/iNOS activity rescues Cav-1_{EC}–$TRPV4_{EC}$ signaling, improves vasodilation, and lowers PAP in PH. These results identify a pathological mechanism that could be targeted for rescuing endothelial Ca^{2+} signaling and vasodilation in PH.

Materials and Methods

Animal Protocols. All animal protocols were approved by the University of Virginia Animal Care and Use Committee (protocols 4,100 and 4,120). Both male and female mice were used in this study. Comparison groups were age and sex matched. A total of 247 mice were used in the study. C57BL6/J were obtained from the Jackson Laboratory. $TRPV4_{EC}^{-/-}$, SMC-specific TRPV4 channel knockout ($TRPV4_{SMC}^{-/-}$), Cav-$1_{EC}^{-/-}$, $iNOS^{-/-}$, and $NOX1^{-/-}$ knockout mice (10 to 14 wk old) were used. Mice were euthanized with pentobarbital (90 mg/kg^{-1} i.p.; Diamondback Drugs) followed by cranial dislocation for harvesting lung tissue. Fourth-order PAs (~50 μm diameter) were isolated in cold Hepes-buffered physiological salt solution (Hepes-PSS, in millimoles per

PHYSIOLOGY

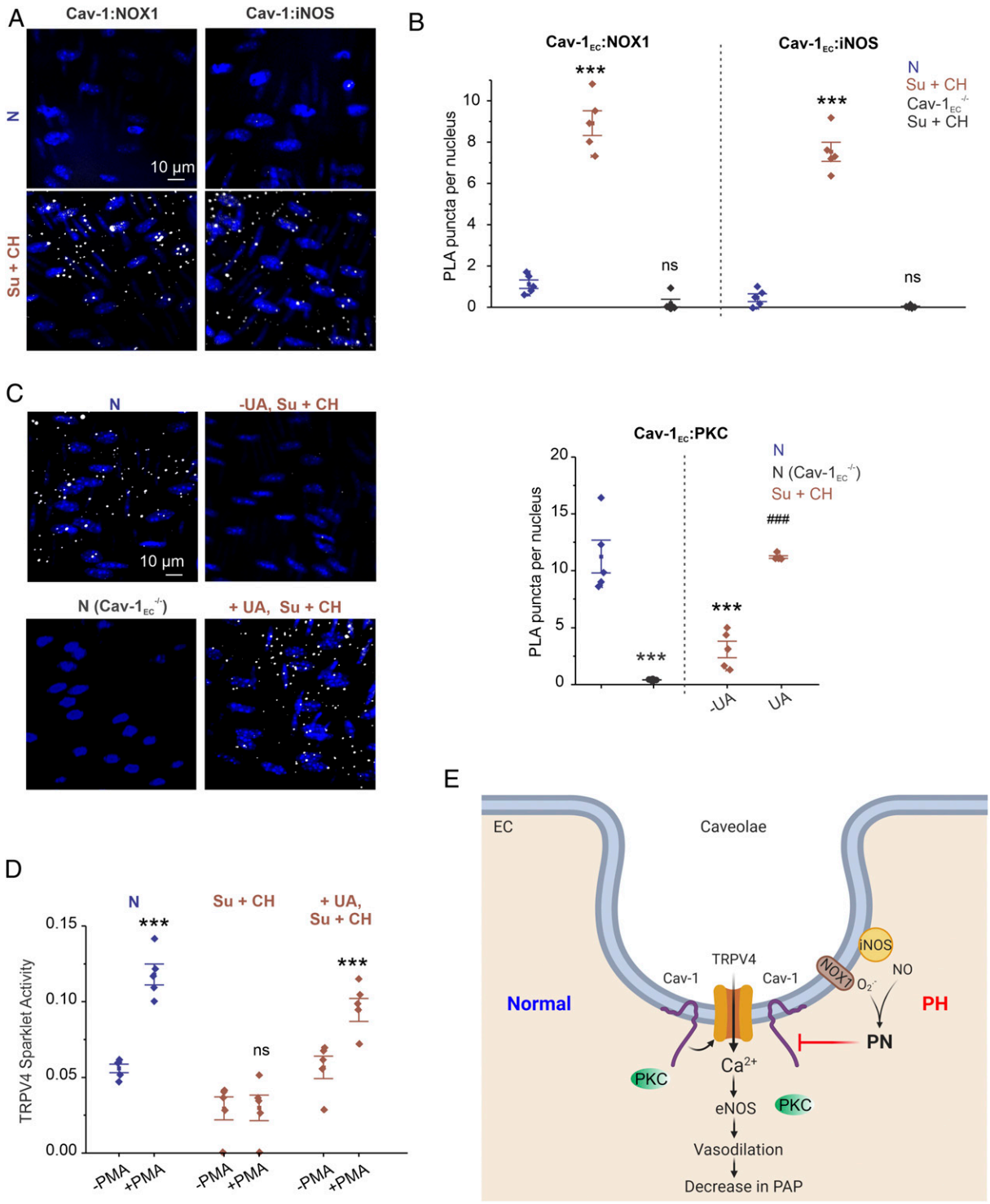

Fig. 8. Colocalization of endothelial NOX1 and iNOS with Cav-1_{EC} impairs Cav-1_{EC}:PKC interaction in PH. (*A*) Representative merged images of PLA showing EC nuclei and Cav-1:NOX1 (*Left*) or Cav-1:iNOS (*Right*) colocalization in fourth-order PAs from mice treated with N or CH (3 wk; 10% O_2) + SU5416. (*B*) Quantification of Cav-1:NOX1 and Cav-1:iNOS colocalization in PAs of N and Su+CH mice and Cav-$1_{EC}^{-/-}$ mice treated with Su+CH ($n = 5$; ***$P < 0.001$ versus N; two-way ANOVA). (*C*, *Left*) Representative merged images of PLA showing EC nuclei and Cav-1_{EC}:PKC colocalization in PAs from N mice (*Top Left*), N Cav-$1_{EC}^{-/-}$ mice (*Bottom Left*), and Su+CH mice in the absence (*Top Right*) or presence (*Bottom Right*) of UA (PN scavenger; 200 μmol/L). (*Right*) Quantification of Cav-1_{EC}:PKC colocalization in PAs from N mice, N Cav-$1_{EC}^{-/-}$ mice, and Su+CH mice in the absence or presence of UA (200 μmol/L; $n = 5$; ***$P < 0.001$ versus N; ###$P < 0.001$ versus Su+CH [−UA]; two-way ANOVA). (*D*) TRPV4$_{EC}$ sparklet activity in PAs from mice treated with N, Su+CH, or Su+CH + UA (200 μmol/L) in the absence or presence of Phorbol 12-myristate 13-acetate (PMA, PKC activator; 10 nmol/L), expressed as NP_O per site ($n = 5$; ***$P < 0.001$ versus N [−PMA]; ***$P < 0.001$ versus Su+CH + UA [−PMA]). (*E*) Schematic depiction of the PN-dependent impairment of endothelial function in PH. TRPV4$_{EC}$ channel-dependent vasodilation reduces PAP. Cav-1_{EC} enhances TRPV4$_{EC}$ channel activity via its interaction with PKC. Up-regulation of iNOS and NOX1 enzymes in caveolae results in increased PN formation in PH. PN, in turn, disrupts Cav-1_{EC}:PKC localization, impairs TRPV4$_{EC}$ channel signaling and vasodilation, and increases PAP in PH.

liter, 10 Hepes, 134 NaCl, 6 KCl, 1 $MgCl_2$ hexahydrate, 2 $CaCl_2$ dihydrate, and 7 dextrose, pH adjusted to 7.4 using 1 mol/L NaOH).

Study Approval for Human PAs. Deidentified lung tissue samples from patients of scleroderma PAH (3 samples) and non-PAH individuals (3 samples) were obtained in accordance with the University of Virginia Institutional Review Board (IRB #19044) and the University of Pittsburgh Committee for Oversight of Research and Clinical Training Involving Descents. Small PAs (~50 μm) were used for pressure myography and Ca^{2+} imaging experiments.

Mouse Models of PH. Two different mouse models of PH were used in this study: CH (10% O_2) for 3 wk or CH with SU5416 [20 mg/kg; subcutaneously; once a week (26) for 3 wk]. SU5416 was dissolved in DMSO. Mice were exposed to CH conditions in a vinyl hypoxic chamber (Coy Laboratory Products, Inc.) connected to an autopurge airlock inlet. The oxygen concentration in the glove box was regulated by an oxygen controller and oxygen sensor (Coy Laboratory Products, Inc.). Control mice were maintained in room air for 3 wk.

Generation of $TRPV4_{EC}^{-/-}$, $Cav\text{-}1_{EC}^{-/-}$, and $TRPV4_{SMC}^{-/-}$ Mice. $TRPV4^{fl/fl}$ (57) and $Cav\text{-}1^{fl/fl}$ (10, 58, 59) mice were crossed with VE-Cadherin (Cdh5, endothelial) Cre mice (60) or SMMHC (smooth muscle) Cre mice (61). EC- or SMC-specific knockout of TRPV4 or Cav-1 was induced by injecting 6 wk old $TRPV4^{fl/fl}$ Cre^{+} or $Cav\text{-}1^{fl/fl}$ Cre^{+} mice with tamoxifen (40 mg/kg per day for 10 d; i.p.). Tamoxifen-injected $TRPV4^{fl/fl}$ Cre^{-} and $Cav\text{-}1^{fl/fl}$ Cre^{-} mice were used as controls. Mice were used for experiments after a 2 wk tamoxifen washout period.

Measurement of PAP and RVSP. PAP was evaluated using an IPL-1 ex vivo murine lung perfusion system (Harvard Apparatus), as previously described (62). RVSP was measured in anesthetized mice using a Mikro Tip pressure catheter (Millar Instruments).

Statistics. Results are presented as mean ± SEM. Data were analyzed using two-tailed paired or independent *t* test (for comparison of data collected from two different treatments) and one-way ANOVA or two-way ANOVA (to investigate statistical differences among more than two different treatments). Statistical significance was determined as a *P* value less than 0.05.

Data Availability. All study data are included in the article and/or *SI Appendix*.

ACKNOWLEDGMENTS. This work was supported by a predoctoral fellowship from the American Heart Association to M.O. (20PRE35210176) and grants from the NIH to E.A.G. (HL113178 and HL130261) and S.K.S. (HL146914, HL142808, and HL147555). We thank Dr. Wolfgang Liedtke (Duke University) for the $TRPV4^{fl/fl}$ mice.

1. S. Rich, S. G. Haworth, P. M. Hassoun, M. H. Yacoub, Pulmonary hypertension: The unaddressed global health burden. *Lancet Respir. Med.* **6**, 577–579 (2018).
2. R. Budhiraja, R. M. Tuder, P. M. Hassoun, Endothelial dysfunction in pulmonary hypertension. *Circulation* **109**, 159–165 (2004).
3. M. Ottolini *et al*., Mechanisms underlying selective coupling of endothelial Ca^{2+} signals with eNOS versus IK/SK channels in systemic and pulmonary arteries. *J. Physiol.* **598**, 3577–3596 (2020).
4. C. Marziano *et al*., Nitric oxide-dependent feedback loop regulates transient receptor potential vanilloid 4 (TRPV4) channel cooperativity and endothelial function in small pulmonary arteries. *J. Am. Heart Assoc.* **6**, e007157 (2017).
5. Y. Xia *et al*., TRPV4 channel contributes to serotonin-induced pulmonary vasoconstriction and the enhanced vascular reactivity in chronic hypoxic pulmonary hypertension. *Am. J. Physiol. Cell Physiol.* **305**, C704–C715 (2013).
6. P. N. Bernatchez *et al*., Dissecting the molecular control of endothelial NO synthase by caveolin-1 using cell-permeable peptides. *Proc. Natl. Acad. Sci. U.S.A.* **102**, 761–766 (2005).
7. F. R. Bakhshi *et al*., Nitrosation-dependent caveolin 1 phosphorylation, ubiquitination, and degradation and its association with idiopathic pulmonary arterial hypertension. *Pulm. Circ.* **3**, 816–830 (2013).
8. N. A. Maniatis *et al*., Increased pulmonary vascular resistance and defective pulmonary artery filling in caveolin-1-/- mice. *Am. J. Physiol. Lung Cell. Mol. Physiol.* **294**, L865–L873 (2008).
9. N. P. Nickel *et al*., Elafin reverses pulmonary hypertension via caveolin-1-dependent bone morphogenetic protein signaling. *Am. J. Respir. Crit. Care Med.* **191**, 1273–1286 (2015).
10. S. D. S. Oliveira *et al*., Injury-induced shedding of extracellular vesicles depletes endothelial cells of Cav-1 (caveolin-1) and enables TGF-β (transforming growth factor-β)-dependent pulmonary arterial hypertension. *Arterioscler. Thromb. Vasc. Biol.* **39**, 1191–1202 (2019).
11. Y.-Y. Zhao *et al*., Defects in caveolin-1 cause dilated cardiomyopathy and pulmonary hypertension in knockout mice. *Proc. Natl. Acad. Sci. U.S.A.* **99**, 11375–11380 (2002).
12. J. Saliez *et al*., Role of caveolar compartmentation in endothelium-derived hyperpolarizing factor-mediated relaxation: Ca2+ signals and gap junction function are regulated by caveolin in endothelial cells. *Circulation* **117**, 1065–1074 (2008).
13. Z. Daneva, V. E. Laubach, S. K. Sonkusare, Novel regulators and targets of redox signaling in pulmonary vasculature. *Curr. Opin. Physiol.* **9**, 87–93 (2019).
14. D. J. R. Fulton *et al*., Reactive oxygen and nitrogen species in the development of pulmonary hypertension. *Antioxidants (Basel)* **6**, 54 (2017).
15. S. Carnesecchi *et al*., NADPH oxidase-1 plays a crucial role in hyperoxia-induced acute lung injury in mice. *Am. J. Respir. Crit. Care Med.* **180**, 972–981 (2009).
16. D. S. de Jesus *et al*., Nox1/Ref-1-mediated activation of CREB promotes Gremlin1-driven endothelial cell proliferation and migration. *Redox Biol.* **22**, 101138 (2019).
17. I. A. Ghouleh *et al*., Endothelial Nox1 oxidase assembly in human pulmonary arterial hypertension; Driver of Gremlin1-mediated proliferation. *Clin. Sci. (Lond.)* **131**, 2019–2035 (2017).
18. K. Suresh *et al*., Reactive oxygen species induced Ca^{2+} influx via TRPV4 and microvascular endothelial dysfunction in the SU5416/hypoxia model of pulmonary arterial hypertension. *Am. J. Physiol. Lung Cell. Mol. Physiol.* **314**, L893–L907 (2018).
19. R. Radi, J. S. Beckman, K. M. Bush, B. A. Freeman, Peroxynitrite oxidation of sulfhydryls. The cytotoxic potential of superoxide and nitric oxide. *J. Biol. Chem.* **266**, 4244–4250 (1991).
20. R. Bowers *et al*., Oxidative stress in severe pulmonary hypertension. *Am. J. Respir. Crit. Care Med.* **169**, 764–769 (2004).
21. M. Ottolini *et al*., Local peroxynitrite impairs endothelial transient receptor potential vanilloid 4 channels and elevates blood pressure in obesity. *Circulation* **141**, 1318–1333 (2020).
22. V. Hampl *et al*., Pulmonary vascular iNOS induction participates in the onset of chronic hypoxic pulmonary hypertension. *Am. J. Physiol. Lung Cell. Mol. Physiol.* **290**, L11–L20 (2006).
23. T. Hoehn, B. Stiller, A. R. McPhaden, R. M. Wadsworth, Nitric oxide synthases in infants and children with pulmonary hypertension and congenital heart disease. *Respir. Res.* **10**, 110 (2009).
24. S. K. Sonkusare *et al*., Elementary Ca2+ signals through endothelial TRPV4 channels regulate vascular function. *Science* **336**, 597–601 (2012).
25. H.-C. Fan, X. Zhang, P. A. McNaughton, Activation of the TRPV4 ion channel is enhanced by phosphorylation. *J. Biol. Chem.* **284**, 27884–27891 (2009).
26. S. H. Vitali *et al*., The Sugen 5416/hypoxia mouse model of pulmonary hypertension revisited: Long-term follow-up. *Pulm. Circ.* **4**, 619–629 (2014).
27. N. L. Jernigan *et al*., Contribution of reactive oxygen species to the pathogenesis of pulmonary arterial hypertension. *PLoS One* **12**, e0180455 (2017).
28. Y. Ravi *et al*., Pulmonary hypertension secondary to left-heart failure involves peroxynitrite-induced downregulation of PTEN in the lung. *Hypertension* **61**, 593–601 (2013).
29. J. R. Klinger, S. H. Abman, M. T. Gladwin, Nitric oxide deficiency and endothelial dysfunction in pulmonary arterial hypertension. *Am. J. Respir. Crit. Care Med.* **188**, 639–646 (2013).
30. M. Cheung *et al*., Discovery of GSK2193874: An orally active, potent, and selective blocker of transient receptor potential vanilloid 4. *ACS Med. Chem. Lett.* **8**, 549–554 (2017).
31. W. M. Kuebler, S.-E. Jordt, W. B. Liedtke, Urgent reconsideration of lung edema as a preventable outcome in COVID-19: Inhibition of TRPV4 represents a promising and feasible approach. *Am. J. Physiol. Lung Cell. Mol. Physiol.* **318**, L1239–L1243 (2020).
32. M. T. Lin *et al*., Functional coupling of TRPV4, IK, and SK channels contributes to Ca(2+)-dependent endothelial injury in rodent lung. *Pulm. Circ.* **5**, 279–290 (2015).
33. E. A. Pankey, A. Zsombok, G. F. Lasker, P. J. Kadowitz, Analysis of responses to the TRPV4 agonist GSK1016790A in the pulmonary vascular bed of the intact-chest rat. *Am. J. Physiol. Heart Circ. Physiol.* **306**, H33–H40 (2014).
34. E. Martin *et al*., Involvement of TRPV1 and TRPV4 channels in migration of rat pulmonary arterial smooth muscle cells. *Pflugers Arch.* **464**, 261–272 (2012).
35. S. Song *et al*., Flow shear stress enhances intracellular Ca2+ signaling in pulmonary artery smooth muscle cells from patients with pulmonary arterial hypertension. *Am. J. Physiol. Cell Physiol.* **307**, C373–C383 (2014).
36. X.-R. Yang *et al*., Upregulation of osmo-mechanosensitive TRPV4 channel facilitates chronic hypoxia-induced myogenic tone and pulmonary hypertension. *Am. J. Physiol. Lung Cell. Mol. Physiol.* **302**, L555–L568 (2012).
37. M. Ottolini, K. Hong, S. K. Sonkusare, Calcium signals that determine vascular resistance. *Wiley Interdiscip. Rev. Syst. Biol. Med.* **11**, e1448 (2019).
38. K. Hong *et al*., TRPV4 (transient receptor potential vanilloid 4) channel-dependent negative feedback mechanism regulates G_q protein-coupled receptor-induced vasoconstriction. *Arterioscler. Thromb. Vasc. Biol.* **38**, 542–554 (2018).
39. M. A. El-Brolosy, D. Y. R. Stainier, Genetic compensation: A phenomenon in search of mechanisms. *PLoS Genet.* **13**, e1006780 (2017).
40. D. F. Alvarez *et al*., Transient receptor potential vanilloid 4-mediated disruption of the alveolar septal barrier: A novel mechanism of acute lung injury. *Circ. Res.* **99**, 988–995 (2006).
41. K. Hamanaka *et al*., TRPV4 channels augment macrophage activation and ventilator-induced lung injury. *Am. J. Physiol. Lung Cell. Mol. Physiol.* **299**, L353–L362 (2010).
42. Y. Jia *et al*., Functional TRPV4 channels are expressed in human airway smooth muscle cells. *Am. J. Physiol. Lung Cell. Mol. Physiol.* **287**, L272–L278 (2004).

PHYSIOLOGY

43. I. M. Lorenzo, W. Liedtke, M. J. Sanderson, M. A. Valverde, TRPV4 channel participates in receptor-operated calcium entry and ciliary beat frequency regulation in mouse airway epithelial cells. *Proc. Natl. Acad. Sci. U.S.A.* **105**, 12611–12616 (2008).
44. K. S. Thorneloe *et al*., An orally active TRPV4 channel blocker prevents and resolves pulmonary edema induced by heart failure. *Sci. Transl. Med.* **4**, 159ra148 (2012).
45. J. Yin *et al*., Negative-feedback loop attenuates hydrostatic lung edema via a cGMP-dependent regulation of transient receptor potential vanilloid 4. *Circ. Res.* **102**, 966–974 (2008).
46. T. Stevens, Functional and molecular heterogeneity of pulmonary endothelial cells. *Proc. Am. Thorac. Soc.* **8**, 453–457 (2011).
47. T. A. Longden *et al*., Capillary K^+-sensing initiates retrograde hyperpolarization to increase local cerebral blood flow. *Nat. Neurosci.* **20**, 717–726 (2017).
48. S. A. Mendoza *et al*., TRPV4-mediated endothelial Ca2+ influx and vasodilation in response to shear stress. *Am. J. Physiol. Heart Circ. Physiol.* **298**, H466–H476 (2010).
49. R. Köhler *et al*., Evidence for a functional role of endothelial transient receptor potential V4 in shear stress-induced vasodilatation. *Arterioscler. Thromb. Vasc. Biol.* **26**, 1495–1502 (2006).
50. V. Hartmannsgruber *et al*., Arterial response to shear stress critically depends on endothelial TRPV4 expression. *PLoS One* **2**, e827 (2007).
51. S. Gödecke *et al*., Thrombin-induced ATP release from human umbilical vein endothelial cells. *Am. J. Physiol. Cell Physiol.* **302**, C915–C923 (2012).
52. Y.-Y. Zhao *et al*., Persistent eNOS activation secondary to caveolin-1 deficiency induces pulmonary hypertension in mice and humans through PKG nitration. *J. Clin. Invest.* **119**, 2009–2018 (2009).
53. H. R. Heathcote *et al*., Endothelial TRPV4 channels modulate vascular tone by Ca^{2+}-induced Ca^{2+} release at inositol 1,4,5-trisphosphate receptors. *Br. J. Pharmacol.* **176**, 3297–3317 (2019).
54. M. Madesh *et al*., Selective role for superoxide in InsP3 receptor-mediated mitochondrial dysfunction and endothelial apoptosis. *J. Cell Biol.* **170**, 1079–1090 (2005).
55. C. Bogdan, Nitric oxide synthase in innate and adaptive immunity: An update. *Trends Immunol.* **36**, 161–178 (2015).
56. R. Radi, Peroxynitrite, a stealthy biological oxidant. *J. Biol. Chem.* **288**, 26464–26472 (2013).
57. C. Moore *et al*., UVB radiation generates sunburn pain and affects skin by activating epidermal TRPV4 ion channels and triggering endothelin-1 signaling. *Proc. Natl. Acad. Sci. U.S.A.* **110**, E3225–E3234 (2013).Corrected in: *Proc. Natl. Acad. Sci. U.S.A.* **110**, 15502 (2013).
58. Z. Chen *et al*., Reciprocal regulation of eNOS and caveolin-1 functions in endothelial cells. *Mol. Biol. Cell* **29**, 1190–1202 (2018).
59. S. D. S. Oliveira *et al*., Inflammation-induced caveolin-1 and BMPRII depletion promotes endothelial dysfunction and TGF-β-driven pulmonary vascular remodeling. *Am. J. Physiol. Lung Cell. Mol. Physiol.* **312**, L760–L771 (2017).
60. I. Sörensen, R. H. Adams, A. Gossler, DLL1-mediated Notch activation regulates endothelial identity in mouse fetal arteries. *Blood* **113**, 5680–5688 (2009).
61. A. Wirth *et al*., G12-G13-LARG-mediated signaling in vascular smooth muscle is required for salt-induced hypertension. *Nat. Med.* **14**, 64–68 (2008). Correction in: *Nat. Med.* **14**, 222 (2008).
62. F. Anvari *et al*., Tissue-derived proinflammatory effect of adenosine A2B receptor in lung ischemia-reperfusion injury. *J. Thorac. Cardiovasc. Surg.* **140**, 871–877 (2010).
63. S. K. Sonkusare *et al*., AKAP150-dependent cooperative TRPV4 channel gating is central to endothelium-dependent vasodilation and is disrupted in hypertension. *Sci. Signal.* **7**, ra66 (2014).